# Near-field characteristics of circular piston radiators with simple support

Cheng He and Alex E. Hay
*Department of Physics, Memorial University of Newfoundland, St. John's, Newfoundland A1B 3X7, Canada*

(Received 15 August 1992; revised 2 March 1993; accepted 15 March 1993)

A closed-form expression for the pressure field produced by a circular piston radiator with simply supported boundary condition and continuous-wave excitation is derived. The method of Hasegawa *et al.* [J. Acoust. Soc. Am. **74**, 1044–1047 (1983)], developed for a uniformly vibrating piston, is extended to include the nonuniform case. The resulting expression is valid for all field points and for large ratio of source diameter to wavelength. The average pressure on the surface of a circular receiver as a function of receiver size and distance from the transducer is also calculated.

PACS numbers: 43.20.Rz, 43.20.Tb, 43.40.Rj

## INTRODUCTION

The problem of the baffled circular radiator has been very widely studied for various applications. A complete description of the sound field produced by an acoustic radiator can be obtained from the Rayleigh integral[1]

$$\varphi=\frac{1}{2\pi}\int_s \frac{ve^{-ikR}}{R}\,ds, \tag{1}$$

where $\varphi$, $R$, and $v$ are, respectively, the velocity potential, the distance from the observation point to the radiator surface element $ds$, and the normal velocity at the surface of the radiator.

Because of the complex nature of the beam pattern close to the source, the integration of the equation for pressure becomes very difficult to perform explicitly. Therefore, numerical techniques are usually required.[2–5] Analytical solutions for particular cases are always valuable, however, providing useful comparisons with numerical results, and instructive physical insight into the behavior of the sound field as a function of system parameters.

For real situations, the velocity on the surface of the radiator may not be uniform. If the crystal displacement is dominated by the first mode of vibration (i.e., the only nodal circle on the vibrating surface is at the edge), the velocity on the surface of the piston should increase from the edge to the center, the maximum being at the center.[6] This is the simplest case of nonuniform vibration, and is the one treated here. Dekker *et al.*[7] and Greenspan[8] considered two different cases: (1) a disk with simply supported edges, for which radial vibration of the disk is everywhere possible and only axial displacements vanish at the edge of the disk; and (2) a disk with clamped edges, for which both the radial and axial displacements vanish at the clamped boundary. For the case of simple support, the velocity distribution on the surface of the piston can be expressed in the form

$$v=V_0[1-(r/a)^2]. \tag{2}$$

For the clamped case, this becomes

$$v=V_0[1-(r/a)^2]^2. \tag{3}$$

Dekker *et al.* and Greenspan obtained closed-form expressions for the sound pressure amplitude or intensity along the axis. Hasegawa *et al.*[9,10] obtained a rigorous expression for the field at any point produced by a circular piston source, but only for the uniformly vibrating case.

Up to now, however, no closed-form expression for the acoustical pressure in the whole nearfield, including nonuniform velocity distribution on the source surface, has appeared in the literature. Based on the work of Hasegawa *et al.*,[9,10] this paper presents the derivation of such a formula for the near-field sound pressure of a circular piston undergoing continuous wave excitation. The results for the case of nonuniform surface velocity are compared with those for the uniform case.

## I. GENERAL THEORY

### A. Uniform radiator case

Because some results from Hasegawa *et al.*[9,10] will be used later, in this section we briefly review their work.

Two coordinate systems are used, as shown in Fig. 1: the cylindrical coordinates $(z,\rho,\phi)$, coaxial with the piston; and the spherical coordinate system $(r,\theta,\phi)$ centered at $z=r_0$ on the axis of symmetry. In Eq. (1), $R$ is given by

$$R^2=r^2+r_1^2-2rr_1\cos\Gamma, \tag{4}$$

where

$$\cos\Gamma=\cos\theta\cos\theta_1+\sin\theta\sin\theta_1\cos(\phi-\phi_1). \tag{5}$$

It can be shown[9] that

$$\frac{e^{-ikR}}{R}=-ik\sum_{n=0}^{\infty}(2n+1)j_n(kr)h_n^{(2)}(kr_1)P_n(\cos\Gamma),\quad r<r_1, \tag{6}$$

where $j_n$, $h_n^{(2)}$, and $P_n$ are, respectively, the $n$th-order spherical Bessel function, spherical Hankel function of the

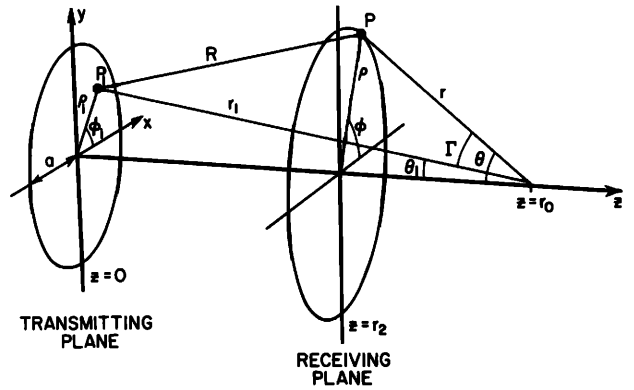


FIG. 1. Coordinate system.

second kind, and Legendre polynomial. Equation (1) can then be rewritten as

$$\varphi(r,\theta)=-ik\sum_{n=0}^{\infty}(2n+1)j_n(kr)\int\int_{s_1}h_n^{(2)}(kr_1)\times P_n(\cos\Gamma)ds_1, \quad (7)$$

where $v$ has been set equal to unity, corresponding to the case of uniform vibration. Note that $ds_1=r_1\,dr_1\,d\phi_1$, since

$$r_1^2=\rho_1^2+r_0^2. \quad (8)$$

According to the addition theorem[11] for Legendre polynomials, it follows that

$$P_n(\cos\Gamma)=P_n(\cos\theta)P_n(\cos\theta_1)+2\sum_{m=1}^{n}\frac{(n-m)!}{(n+m)!}\times P_n^m(\cos\theta)P_n^m(\cos\theta_1)\cos(\phi-\phi_1), \quad (9)$$

where $P_n^m$ is the associated Legendre function of the first kind. Integrating both sides of the above equation with respect to $\phi_1$ gives

$$\int_0^{2\pi}P_n(\cos\Gamma)d\phi_1=2\pi P_n(\cos\theta)P_n(\cos\theta_1). \quad (10)$$

Therefore Eq. (7) becomes:

$$\varphi(r,\theta)=\frac{-2\pi i}{k}\sum_{n=0}^{\infty}(2n+1)j_n(kr)P_n(\cos\theta)\times f_n(Z_0,Z_a), \quad (11)$$

where $Z_0=kr_0$, $Z_a=kr_a$, and $r_a$ is the distance from the rim of the transducer to the origin of the spherical coordinate system, and

$$f_n(Z_0,Z_a)=A_n(Z_a)-A_n(Z_0). \quad (12)$$

The $A_n$ are given by the indefinite integral

$$A_n(Z)=\int Zh_n^{(2)}(Z)P_n\left(\frac{Z_0}{Z}\right)dZ, \quad (13)$$

where $Z=kr_1$. As shown by Hasegawa *et al.*,[9,10] the $A_n$ must satisfy the recurrence relations

$$A_n(Z)=-ZP_n\left(\frac{Z_0}{Z}\right)h_{n-1}^{(2)}(Z)+\sum_{m=1}^{[n/2]}(-1)^{m+1}\times(2n-4m+1)P_{n-2m}\left(\frac{Z_0}{Z}\right)h_{n-2m}^{(2)}(Z),\quad n\geqslant 2, \quad (14)$$

$$A_n(Z)+A_{n-2}(Z)=-Zh_{n-1}^{(2)}(Z)\left[P_n\left(\frac{Z_0}{Z}\right)-P_{n-2}\left(\frac{Z_0}{Z}\right)\right], \quad (15)$$

$$A_n(Z_0)+A_{n-2}(Z_0)=0, \quad (16)$$

where $[n/2]$ means the integer part of $n/2$.

For a piston with a uniform velocity distribution, the above formulas can be used for calculating the acoustical pressure distribution in the near field, and Hasegawa *et al.* used it to compute the three-dimensional pressure field. However, the boundary conditions imposed upon the crystal are one factor which will affect the velocity distribution. We consider this problem below.

### B. Simply supported radiator

Now we consider the problem of nonuniform velocity distribution on the surface of the radiator. This may, in some applications, be more realistic. In the case of ultrasonic transducers, experimental evidence indicates that the surface velocity has a nonuniform distribution rather than a uniform distribution.[7,12,13]

Laura[6] discussed the far-field beampattern produced by circular radiators with two different normal velocity profiles at the surface. For the simply supported case, the surface velocity is given by the expression

$$v(\rho_1)=\sum_{n=1}^{N}d_n\left[1-\left(\frac{\rho_1}{a_1}\right)^{2n}\right], \quad (17)$$

where the $d_n$ are constants representing the weights for the different vibrational modes. For the clamped case,

$$v(\rho_1)=\sum_{n=2}^{N}c_n\left[1-\left(\frac{\rho_1}{a_1}\right)^2\right]^{2n}. \quad (18)$$

Here, $c_n$ have the same meaning as the $d_n$.

Dekker *et al.*[7] and Greenspan[8] have computed the sound pressure distribution on the acoustic axis, and their results indicate that the on-axis pressure distribution is similar for these two different cases. In this paper we therefore consider only the simply supported case, treating it as an example. The result for the clamped plate can be obtained in a similar way.

The following analysis is based on the assumption that the first mode of vibration dominates the crystal displacement. So the velocity distribution on the disk surface can be approximately expressed by

$$v(\rho_1)=\begin{cases}V_0(1-\rho_1^2/a_1^2), & \rho_1<a_1,\\ 0, & \rho_1\geqslant a_1.\end{cases} \quad (19)$$

Here, $v$ is the surface normal velocity as before and $V_0$ is the surface velocity at the transmitter center, which is assumed to be unity. Using Eqs. (8) and (10), the relative velocity potential at the point $P$ is now:

$$\varphi(r,\theta)=\int\int_{s_1}\frac{[(1+r_0^2/a_1^2)-r_1^2/a_1^2]}{R}e^{-ikR}\,ds_1$$

$$=-2\pi ki\sum_{n=0}^{\infty}(2n+1)j_n(kr)P_n(\cos\theta)$$

$$\times\left[\left(1+\frac{r_0^2}{a_1^2}\right)\int_{r_0}^{r_a}h_n^{(2)}(kr_1)P_n\left(\frac{r_0}{r_1}\right)r_1\,dr_1\right.$$

$$\left.-\int_{r_0}^{r_a}\frac{r_1^3}{a_1^2}h_n^{(2)}(kr_1)P_n\left(\frac{r_0}{r_1}\right)dr_1\right]. \quad (20)$$

If we let $Z=kr_1$ as before and define $B_n(Z)$

$$B_n(Z)=\int Z^3h_n^{(2)}(Z)P_n\left(\frac{Z_0}{Z}\right)dZ, \quad (21)$$

in analogy with Eq. (13), then

$$B_n(Z_a)-B_n(Z_0)=\int_{Z_0}^{Z_a}Z^3h_n^{(2)}(Z)P_n\left(\frac{Z_0}{Z}\right)dZ, \quad (22)$$

where $Z_0=kr_0$ and $Z_a=kr_a$ as before. Equation (20) can then be rewritten as

$$\varphi(r,\theta)=\frac{-2\pi i}{k}\sum_{n=0}^{\infty}(2n+1)j_n(kr)P_n(\cos\theta)\left[\left(1+\frac{r_0^2}{a_1^2}\right)\right.$$

$$\left.\times f_n(Z_0,Z_a)-\frac{1}{a_1^2k^2}b_n(Z_0,Z_a)\right], \quad (23)$$

where

$$b_n(Z_0,Z_a)=k^4\int_{r_0}^{r_a}r_1^3h_n^{(2)}(kr_1)P_n\left(\frac{r_0}{r_1}\right)dr_1. \quad (24)$$

The velocity potential $\varphi$ now consists of two parts. The first part can be seen to correspond to the expression for the uniform velocity case, Eq. (11). The second part is the modifying term caused by the nonuniform velocity on the piston surface. Equation (21) can be integrated by parts, using the relations[11]

$$Zh_n^{(2)}(Z)=(2n-1)h_{n-1}^{(2)}(Z)-Zh_{n-2}^{(2)}(Z), \quad (25)$$

$$(n+1)P_{n+1}(Z)-(2n+1)ZP_n(Z)+nP_{n-1}(Z)=0, \quad (26)$$

and

$$\int Z^{1-n}h_n^{(2)}(Z)dZ=-Z^{1-n}h_{n-1}^{(2)}(Z). \quad (27)$$

Then, the first several successive $B_n(Z)$'s can be obtained analytically (see Appendix A), and are given by

$$B_0(Z)=(-Z^2+i2Z+2)e^{-iZ}, \quad (28)$$

$$B_1(Z)=-Z_0(2+iZ)e^{-iZ}, \quad (29)$$

$$B_2(Z)=Z^2A_2(Z)+3Z_0A_1(Z)-4A_0(Z)+Z^2h_0(Z), \quad (30)$$

$$B_3(Z)=Z^2A_3(Z)+\tfrac{10}{3}Z_0A_2(Z)-\tfrac{26}{3}A_1(Z)$$
$$+\tfrac{4}{3}Z_0Zh_1(Z), \quad (31)$$

$$B_4(Z)=Z^2[A_4(Z)-\tfrac{3}{4}A_2(Z)]-[10A_2(Z)-2A_0(Z)]$$
$$+\tfrac{3}{2}A_0(Z)+\tfrac{7}{2}Z_0A_3(Z)-\tfrac{15}{2}A_2(Z)+\tfrac{3}{4}B_2(Z), \quad (32)$$

$$B_5(Z)=Z^2[A_5(Z)-\tfrac{4}{5}A_3(Z)]-2[7A_3(Z)-3A_1(Z)]$$
$$+\tfrac{24}{5}A_1(Z)+\tfrac{18}{5}Z_0A_4(Z)-\tfrac{56}{5}A_3(Z)+\tfrac{4}{5}B_3(Z), \quad (33)$$

$$B_6(Z)=Z^2[A_6(Z)-\tfrac{5}{6}A_4(Z)]-2[9A_4(Z)-5A_2(Z)$$
$$+A_0(Z)]+2[\tfrac{25}{6}A_2(Z)-\tfrac{5}{6}A_0(Z)]$$
$$+\tfrac{11}{3}Z_0A_5(Z)-15A_4(Z)+\tfrac{5}{6}B_4(Z). \quad (34)$$

Using these equations, the relation below can be obtained by induction,

$$B_n(Z)=Z^2\left(A_n(Z)-\frac{(n-1)}{n}A_{n-2}(Z)\right)-2\sum_{m=1}^{[n/2]}(-1)^{m+1}(2n-4m+1)A_{n-2m}(Z)+\frac{2(n-1)}{n}\sum_{m=1}^{[n/2-1]}(-1)^{m+1}$$
$$\times(2n-4m-3)A_{n-2m-2}(Z)+\frac{2(2n-1)}{n}Z_0A_{n-1}(Z)-\frac{2(n-1)(2n-3)}{n}A_{n-2}(Z)+\frac{n-1}{n}B_{n-2},\quad n>3. \quad (35)$$

The above equation can be further simplified by first letting

$$g_n(Z)=\sum_{m=1}^{[n/2]}(-1)^{m+1}(2n-4m+1)A_{n-2m}(Z),\quad n\geqslant 2, \quad (36)$$

where

$$g_0(Z)=g_1(Z)=0. \quad (37)$$

It then follows that

$$g_{n-2}(Z)=\sum_{m=1}^{[n/2-1]}(-1)^{m+1}(2n-4m-3)A_{n-2m-2}(Z),$$
$$n\geqslant 4, \quad (38)$$

and thus

$$g_n(Z)+g_{n-2}(Z)=(2n-3)A_{n-2}(Z),\quad n\geqslant 2. \quad (39)$$

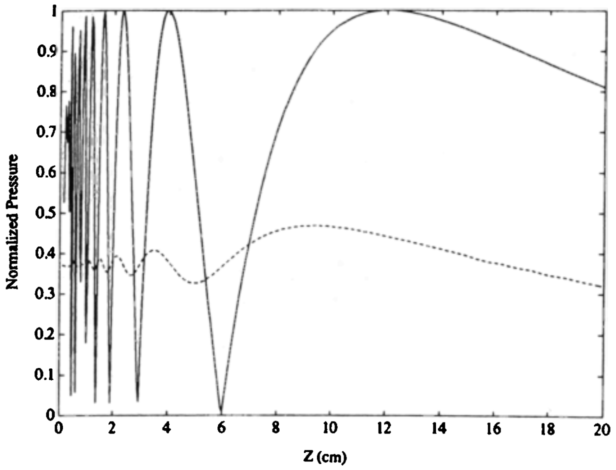


FIG. 2. Acoustical pressure on the acoustical axis, $f=2.0$ MHz.

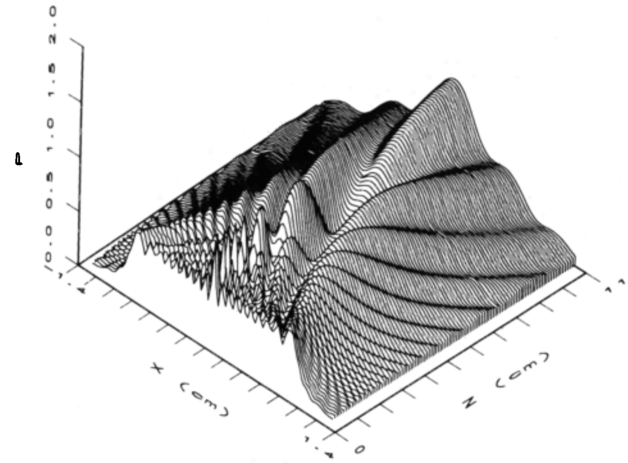

FIG. 3. Three-dimensional pressure distribution, with uniform surface velocity.

Substituting $g_n(Z)$ into Eq. (35) finally gives the recurrence formula for $B_n(Z)$ as

$$B_n(Z)=Z^2\left(A_n(Z)-\frac{(n-1)}{n}A_{n-2}(Z)\right)+\frac{2(2n-1)}{n}$$

$$\times Z_0A_{n-1}(Z)-\frac{2(n-1)(2n-3)}{n}A_{n-2}(Z)$$

$$-2g_n(Z)+\frac{2(n-1)}{n}g_{n-2}(Z)+\frac{n-1}{n}B_{n-2}(Z),$$

$$n>3. \tag{40}$$

The above result can be proved by differentiating both sides with respect to $Z$ (Appendix B). Equation (40), for $n>3$, and Eqs. (28)–(31) for $n\leqslant 3$, express the $B_n(Z)$ as functions of the $A_n(Z)$, given by Eqs. (14)–(16). These relations therefore mean that the velocity potential given by Eq. (23) for the particular case of non-uniform displacements at the transducer surface considered here, can be computed in terms of the coefficients $A_n$ for the uniform case. Since the recurrence formulae can be computed easily and the $B_n(Z)$ converge rapidly, the velocity potential $\varphi(r,\theta)$ can be evaluated efficiently. Because no approximation is used in the derivation, the result should be as exact as specified by the convergence limits.

## II. NEAR FIELD OF A CIRCULAR PLANE RADIATOR

By use of the above equations the acoustical pressure $p[=-\rho_0(d\phi/dt)]$ is calculated for points located on a grid in the $x$-$z$ plane. In our calculation the diameter of the piston is equal to 1.90 cm, the frequency $f=2.0$ MHz, corresponding to a transducer used in a set of scattering experiments described elsewhere.[14] The speed of sound in water is taken to be 1483 m $\text{s}^{-1}$. We chose $r_0=22$ cm.

Figure 2 shows the sound pressure on the acoustical axis (i.e., the $z$ axis). The dashed and solid curves, respectively, are the results with the nonuniform and uniform velocity distribution on the piston surface. It is evident that the extrema in the dashed curve are small compared with those in the solid curve. As well, there are no zeroes in the dashed curve, and its last maximum occurs at a point nearer the piston surface than that of the solid curve, at approximately $0.75a^2/\lambda$. All of these characteristics are in good agreement with the results of Dekker *et al.*[7] and Greenspan.[8]

Figures 3 and 4 are three-dimensional representations of the sound pressure field for uniform and nonuniform $v$, respectively, calculated by using Eqs. (11) and (23). The computations were made in the $z$ direction for $0\leqslant z\leqslant 12$ cm and in the $x$ direction from the center of the circular radiator to 1.4 times the transducer radius. It can be seen that an interference pattern exists in both of them, but Fig. 4 is much more regular and smooth, with sidelobes being essentially absent. These results are similar to those that have been obtained by numerical integration for radially symmetric surface velocity distributions with zero normal velocity at the boundary.[4]

## III. SPATIALLY AVERAGED PRESSURE IN THE NEAR FIELD

Since the output of a receiver is proportional to the average acoustical pressure acting on its surface, in practi-

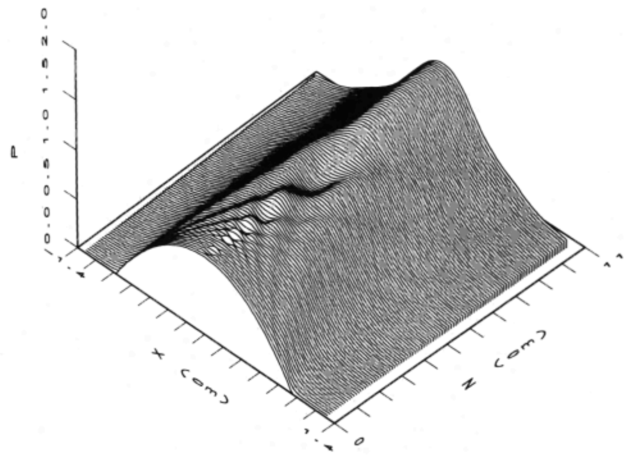

FIG. 4. Three-dimensional pressure distribution, with nonuniform surface velocity.

cal applications, knowing how beamwidth and average pressure on the receiver surface change along the acoustical axis is often important. We will use the formulas obtained above to determine how the acoustical pressure on the plane which is perpendicular to the $z$ axis changes with axial distance. (Here we use pressure instead of velocity potential. The difference between them is just a constant at a given frequency.)

The spatially averaged value of $p$ over the receiving crystal is

$$\langle p\rangle=\frac{1}{s_2}\int\int_{s_2} p\, ds_2, \tag{41}$$

where $s_2$ is the receiving crystal area, and $ds_2=\rho\, d\rho\, d\phi$. From the relation

$$r^2=\rho^2+(r_0-r_2)^2. \tag{42}$$

Then $ds_2$ is

$$ds_2=r\, dr\, d\phi. \tag{43}$$

Substituting Eq. (23) into Eq. (41) gives

$$\langle p\rangle=\frac{-1}{ks_2}\left\{2\pi i\sum_{n=0}^{\infty}(2n+1)\times\left[\left(1+\frac{r_0^2}{a_1^2}\right)f_n(Z_0,Z_1)-\frac{1}{a_1^2k^2}b_n(Z_0,Z_1)\right]\times\int_{r_0-r_2}^{r_{a2}}\int_0^{2\pi}j_n(kr)P_n\left(\frac{r_0-r_2}{r}\right)r\, dr\, d\phi\right\}. \tag{44}$$

The integral can be simplified as follows:

$$\begin{aligned}\int_{r_0-r_2}^{r_{a2}}\int_0^{2\pi}j_n(kr)P_n\left(\frac{r_0-r_2}{r}\right)r\, dr\, d\phi &=\frac{2\pi}{k^2}\int_{k(r_0-r_2)}^{kr_{a2}}Z\,\mathrm{Re}[h_n^{(2)}(Z)]P_n\left(\frac{Z_0'}{Z}\right)dZ\\ &=\frac{2\pi}{k^2}\mathrm{Re}\left[\int_{k(r_0-r_2)}^{kr_{a2}}Zh_n^{(2)}(Z)P_n\left(\frac{Z_0'}{Z}\right)dZ\right]\\ &=\frac{2\pi}{k^2}\mathrm{Re}[f_n(Z_0',Z_1')],\end{aligned} \tag{45}$$

where $Z_0'=k(r_0-r_2)$ and $Z_1'=kr_{a2}$, with $r_{a2}$ being the distance from the rim of the receiving plane to the origin of the spherical coordinate system. Equation (44) then becomes

$$\langle p\rangle=\frac{-1}{s_2k^3}4\pi^2 i\sum_{n=0}^{\infty}(2n+1)\left[\left(1+\frac{r_0^2}{a_1^2}\right)f_n(Z_0,Z_1)-\frac{1}{a_1^2k^2}b_n(Z_0,Z_1)\right]\mathrm{Re}[f_n(Z_0',Z_1')]. \tag{46}$$

Figure 5 shows the values of average relative acoustical pressure on receiving planes of differing sizes as a function axial distance $z$. Figure 6 shows the same results for the case when $v$ is uniform. By comparing Figs. 5 and 6, it is easily seen that the average acoustical pressure on the receiving area along the acoustical axis changes less when the boundary condition for the simply supported radiator is applied. The slopes of the curves in Fig. 6 are also larger than those in Fig. 5, implying greater beam divergence in the uniform case.

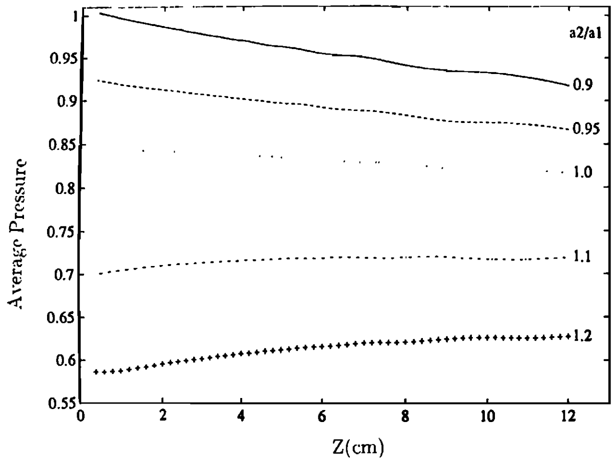


FIG. 5. Average relative pressure on different sized receiving surfaces (radius $a2$) produced by transmitter (radius $a1$) with nonuniform surface velocity, at $f=2.0$ MHz.

## IV. CONCLUSIONS

A closed-form expression has been derived for the sound field produced by a circular piston with nonuniform surface velocity. The expression has the advantages of including no approximations and not requiring numerical integration.

The results for the near-field beam pattern are consistent with those that have been obtained previously by numerical integration.[4] That is, compared to the near-field beam pattern produced by a circular piston with uniform surface velocity, that from a piston with simple support vibrating in the first mode is much less complex, being

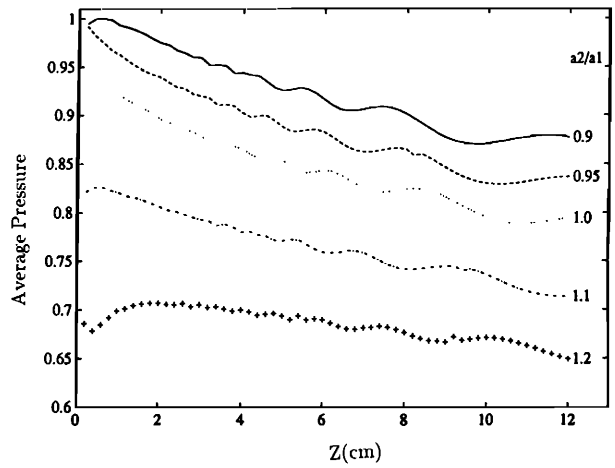


FIG. 6. Average relative pressure on different sized receiving surfaces produced by transmitter with uniform surface velocity, at $f=2.0$ MHz.

essentially free of sidelobes and axial foci. Furthermore, it is shown by computing the average pressure on receiving surfaces of different size that the near-field beam pattern in the nonuniform case approaches the divergence-free limit much more closely than does the uniformly vibrating piston. This appears to be a new result.

The disappearance of the sidelobes and axial foci in the nonuniform case, shown here for the velocity distribution corresponding to the first simply supported mode, and elsewhere for Gaussian and linearly tapered velocity distributions,[4] is clearly related to the fact that the velocity drops monotonically to zero at the boundary in these cases. We suggest that this behaviour can be understood physically in terms of the edge wave/plane wave interference. That is, the beam pattern of a continuous wave uniform piston source can be constructed from the interference between a plane wave propagating from the piston face and an edge wave generated at the piston boundary.[4,15] For the velocity distributions listed above, the amplitude of the edge wave must be considerably reduced compared to the uniform case, and the attendant interference effects therefore largely suppressed.

## APPENDIX A

In order to show how the first several successive $B_n(Z)$ may be obtained, here we give the details associated with calculating $B_2(Z)$ and $B_4(Z)$. The following three relations will be used in the calculation:

$$zh_n^{(2)}(z)=(2n-1)h_{n-1}^{(2)}(z)-zh_{n-2}^{(2)}(z), \tag{A1}$$

$$(n+1)P_{n+1}(z)-(2n+1)zP_n(z)+nP_{n-1}(z)=0, \tag{A2}$$

$$\int z^{1-n}h_n^{(2)}(z)dz=-z^{1-n}h_{n-1}^{(2)}(z). \tag{A3}$$

Then from Hasegawa *et al.*[9] we have

$$A_2(Z)=\int Zh_2^{(2)}(Z)P_2\left(\frac{Z_0}{Z}\right)dZ$$
$$=-ZP_2\left(\frac{Z_0}{Z}\right)h_1^{(2)}(Z)+h_0^{(2)}(Z)$$

and

$$A_4(Z)=\int Zh_4^{(2)}(Z)P_4\left(\frac{Z_0}{Z}\right)dZ$$
$$=-ZP_4\left(\frac{Z_0}{Z}\right)h_3^{(2)}(Z)+5P_2\left(\frac{Z_0}{Z}\right)h_2^{(2)}(Z)-h_0^{(2)}(Z).$$

So,

$$B_2(Z)=\int Z^2\left[Zh_2^{(2)}(Z)P_2\left(\frac{Z_0}{Z}\right)\right]dZ$$
$$=Z^2A_2(Z)-2\int Z\left[-Zh_1^{(2)}(Z)P_2\left(\frac{Z_0}{Z}\right)+h_0^{(2)}(Z)\right]dZ$$
$$=Z^2A_2(Z)-2\int Zh_0^{(2)}(Z)P_0\left(\frac{Z_0}{Z}\right)dZ$$
$$+2\int Z^2h_1^{(2)}\left[\frac{3Z_0}{2Z}P_1\left(\frac{Z_0}{Z}\right)-\frac{1}{2}P_0\left(\frac{Z_0}{Z}\right)\right]dZ$$
$$=Z^2A_2(Z)-2A_0(Z)+3\int ZZ_0h_1^{(2)}(Z)\times P_1\left(\frac{Z_0}{Z}\right)dZ-\int Z^2h_1^{(2)}(Z)\times P_0\left(\frac{Z_0}{Z}\right)dZ$$
$$=Z^2A_2(Z)-2A_0(Z)+3Z_0A_1(Z)+Z^2h_0^{(2)}(Z)-2A_0(Z)$$
$$=Z^2A_2(Z)+3Z_0A_1(Z)-4A_0(Z)+Z^2h_0^{(2)}(Z).$$

Similarly, for $B_4(Z)$

$$B_4(Z)=\int Z^2\left[\left(Zh_4^{(2)}(Z)P_4\left(\frac{Z_0}{Z}\right)\right]dZ$$
$$=Z^2A_4-2\int Z\left[-ZP_4\left(\frac{Z_0}{Z}\right)h_3^{(2)}(Z)+5P_2\left(\frac{Z_0}{Z}\right)h_2^{(2)}(Z)-h_0^{(2)}(Z)\right]dZ$$
$$=Z^2A_4(Z)-10A_2(Z)+2A_0(Z)+2\int Z^2P_4\left(\frac{Z_0}{Z}\right)h_3^{(2)}(Z)dZ$$
$$=Z^2A_4(Z)-10A_2(Z)+2A_0(Z)+2\int Z^2\times h_3^{(2)}(Z)\left[\frac{7Z_0}{4Z}P_3\left(\frac{Z_0}{Z}\right)-\frac{3}{4}P_2\left(\frac{Z_0}{Z}\right)\right]dZ$$
$$=Z^2A_4(Z)-10A_2(Z)+2A_0(Z)+\tfrac{7}{2}Z_0A_3(Z)-\frac{3}{2}\int ZP_2\left(\frac{Z_0}{Z}\right)[5h_2^{(2)}(Z)-Zh_1^{(2)}(Z)]dZ$$
$$=Z^2A_4(Z)-10A_2(Z)+2A_0(Z)+\tfrac{7}{2}Z_0A_3(Z)-\frac{15}{2}A_2(Z)+\frac{3}{2}\int Z^2h_1^{(2)}(Z)P_2\left(\frac{Z_0}{Z}\right)dZ.$$

We know

$$B_2(Z)=Z^2A_2(Z)-2A_0+2\int Z^2h_1^{(2)}(Z)P_2\left(\frac{Z_0}{Z}\right)dZ.$$

Therefore,

$$B_4(Z)=Z^2A_4(Z)-10A_2(Z)+2A_0(Z)+\tfrac{7}{2}Z_0A_3(Z)$$
$$-\tfrac{15}{2}A_2(Z)+\tfrac{3}{4}B_2(Z)-\tfrac{3}{4}[Z^2A_2(Z)-2A_0(Z)]$$
$$=Z^2[A_4(Z)-\tfrac{3}{4}A_2(Z)]-[10A_2(Z)-2A_0(Z)]$$
$$+\tfrac{3}{2}A_0(Z)+\tfrac{7}{2}Z_0A_3(Z)-\tfrac{15}{2}A_2(Z)+\tfrac{3}{4}B_2(Z).$$

Other $B_n(Z)$ may be obtained in a similar way.

## APPENDIX B

Here, we rewrite Eq. (40)

$$B_n(Z)=Z^2\left(A_n(Z)-\frac{(n-1)}{n}A_{n-2}(Z)\right)+\frac{2(2n-1)}{n}\times Z_0A_{n-1}(Z)-\frac{2(n-1)(2n-3)}{n}A_{n-2}(Z)-2g_n(Z)+\frac{2(n-1)}{n}g_{n-2}(Z)+\frac{n-1}{n}B_{n-2}(Z),\quad n>3. \tag{B1}$$

Differentiation of the two sides of Eq. (B1) and using Eq. (21) gives

$$Z^3h_n^{(2)}(Z)P_n\left(\frac{Z_0}{Z}\right)=2Z\left(A_n(Z)-\frac{n-1}{n}A_{n-2}(Z)\right)+Z^3h_n^{(2)}(Z)P_n\left(\frac{Z_0}{Z}\right)-\frac{(n-1)}{n}Z^3h_{n-2}^{(2)}(Z)P_{n-2}\left(\frac{Z_0}{Z}\right)$$
$$+\frac{2(2n-1)}{n}Z_0Zh_{n-1}^{(2)}(Z)P_{n-1}\left(\frac{Z_0}{Z}\right)-\frac{2(n-1)(2n-3)}{n}Zh_{n-2}^{(2)}(Z)P_{n-2}\left(\frac{Z_0}{Z}\right)-2\frac{d}{dZ}g_n(Z)$$
$$+\frac{2(n-1)}{n}\frac{d}{dZ}g_{n-2}(Z)+\frac{n-1}{n}Z^3h_{n-2}^{(2)}(Z)P_{n-2}\left(\frac{Z_0}{Z}\right).$$

Rearranging the above equation and using the relation [Eq. (39)]

$$g_n(Z)+g_{n-2}(Z)=(2n-3)A_{n-2}(Z),$$

we obtain

$$2ZA_n(Z)-\frac{2(n-1)}{n}ZA_{n-2}(Z)+\frac{2(2n-1)}{n}Z_0Zh_{n-1}^{(2)}(Z)\times P_{n-1}\left(\frac{Z_0}{Z}\right)-\frac{2(2n-1)(2n-3)}{n}Zh_{n-2}^{(2)}(Z)\times P_{n-2}\left(\frac{Z_0}{Z}\right)+\frac{2(2n-1)}{n}\frac{d}{dZ}g_{n-2}(Z)=0. \tag{B2}$$

From the relations (14) and (15) for $A_n$ the first two terms in (B2) become

$$2ZA_n(Z)-\frac{2(n-1)}{n}ZA_{n-2}(Z)$$
$$=-2Z^2h_{n-1}^{(2)}(Z)P_n\left(\frac{Z_0}{Z}\right)+2Z^2h_{n-1}^{(2)}(Z)P_{n-2}\left(\frac{Z_0}{Z}\right)-\frac{2(2n-1)}{n}ZA_{n-2}(Z)$$
$$=-2Z^2h_{n-1}^{(2)}(Z)P_n\left(\frac{Z_0}{Z}\right)+2Z^2h_{n-1}^{(2)}(Z)P_{n-2}\left(\frac{Z_0}{Z}\right)+\frac{2(2n-1)}{n}Z^2h_{n-3}^{(2)}(Z)P_{n-2}\left(\frac{Z_0}{Z}\right)$$
$$-\frac{2(2n-1)}{n}Z\sum_{m=1}^{[n/2-1]}(-1)^{m+1}(2n-4m-3)\times h_{n-2m-2}^{(2)}(Z)P_{n-2m-2}\left(\frac{Z_0}{Z}\right)$$
$$=-2Z^2h_{n-1}^{(2)}(Z)P_n\left(\frac{Z_0}{Z}\right)+2Z^2h_{n-1}^{(2)}(Z)P_{n-2}\left(\frac{Z_0}{Z}\right)+\frac{2(2n-1)}{n}Z^2h_{n-3}^{(2)}(Z)P_{n-2}\left(\frac{Z_0}{Z}\right)-\frac{2(2n-1)}{n}\frac{d}{dZ}g_{n-2}. \tag{B3}$$

Using relation

$$nP_n(Z')=(2n-1)Z'P_{n-1}(Z')-(n-1)P_{n-2}(Z'),$$

the first term on the rhs of (B3) can be rewritten as

$$-2Z^2h_{n-1}^{(2)}(Z)P_n\left(\frac{Z_0}{Z}\right)$$
$$=-\frac{2(2n-1)}{n}ZZ_0h_{n-1}^{(2)}(Z)P_{n-1}\left(\frac{Z_0}{Z}\right)+\frac{2(n-1)}{n}Z^2h_{n-1}^{(2)}(Z)P_{n-2}\left(\frac{Z_0}{Z}\right). \tag{B4}$$

Also using the relation

$$Z'h_n^{(2)}(Z')=(2n-1)h_{n-1}^{(2)}(Z')-Z'h_{n-2}^{(2)}(Z'),$$

the third term in (B3) becomes

$$\begin{aligned}\frac{2(2n-1)}{n} & Z^2h_{n-3}^{(2)}(Z)P_{n-2}\left(\frac{Z_0}{Z}\right)\\ &=\frac{2(2n-1)(2n-3)}{n}Zh_{n-2}^{(2)}(Z)P_{n-2}\left(\frac{Z_0}{Z}\right)\\ &\quad-\frac{2(2n-1)}{n}Z^2h_{n-1}^{(2)}(Z)P_{n-2}\left(\frac{Z_0}{Z}\right).\end{aligned}\tag{B5}$$

Substituting Eqs. (B4) and (B5) into (B3), and the resulting equation into Eq. (B2), we find that all terms cancel, proving Eq. (40).


[1] Lord Rayleigh, *The Theory of Sound* (Dover, New York, 1945).

[2] J. Zemanek, "Beam behavior within the nearfield of a vibrating piston," J. Acoust. Soc. Am. **49**, 181–191 (1971).

[3] J. C. Lockwood and J. G. Willette, "High-speed method for computing the exact solution for the pressure variations in the near-field of a baffled piston," J. Acoust. Soc. Am. **53**, 735–741 (1973).

[4] D. A. Hutchins, H. D. Mair, P. A. Puhach, and A. J. Osei, "Continuous-wave pressure field of ultrasonic transducers," J. Acoust. Soc. Am. **80**, 1–12 (1986).

[5] H. D. Mair, L. Bresse, and D. A. Hutchins, "Diffraction effects of planar transducers using a numerical expression for edge waves," J. Acoust. Soc. Am. **84**, 1517–1525 (1988).

[6] P. A. Laura, "Directional characteristics of vibrating circular plates and membranes," J. Acoust. Soc. Am. **40**, 1031–1033 (1966).

[7] L. D. Dekker, R. L. Piziali, and E. Dong, Jr., "Effect of boundary conditions on the ultrasonic-beam characteristics of circular disks," J. Acoust. Soc. Am. **56**, 87–93 (1974).

[8] M. Greenspan, "Piston radiator: some extensions of the theory," J. Acoust. Soc. Am. **65**, 608–621 (1979).

[9] T. Hasegawa, N. Inoue, and K. Matsuzawa, "A new rigorous expansion for the velocity potential of a circular piston source," J. Acoust. Soc. Am. **74**, 1044–1047 (1983).

[10] T. Hasegawa, N. Inoue, and K. Matsuzawa, "Fresnel diffraction: Some extensions of the theory," J. Acoust. Soc. Am. **75**, 1048–1051 (1984).

[11] G. Arfken, *Mathematical Methods for Physicists* (Academic, New York, 1970).

[12] E. A. G. Shaw, "On the resonant vibration of thick barium titanate disks," J. Acoust. Soc. Am. **28**, 38–50 (1956).

[13] E. A. G. Shaw, and R. J. Sujir, "Vibration patterns of loaded barium titanate and quartz discs," J. Acoust. Soc. Am. **32**, 1463–1467 (1960).

[14] C. He, "Broadband Measurements of the Acoustic Backscatter Cross Section of Sand Particles in Suspension," M.S. thesis, Memorial University of Newfoundland (1991).

[15] J. P. Weight and A. J. Hayman, "Observations of the propagation of very short ultrasonic pulses and their reflection by small targets," J. Acoust. Soc. Am. **63**, 396–404 (1978).